Towards large-scale fully-selfconsistent LDA-electronic structure calculations (Order-N Method)

T. Hoshi and T. Fujiwara
Department of Applied Physics, University of Tokyo, Bunkyo-ku, Tokyo 113, Japan

Towards large-scale *ab initio* electronic-structure calculations, we propose a new formalism, where basis orbitals are localized, nonorthogonal, and given on a real-space *regular* grid. A window function is adopted to optimize localized basis orbitals on a real-space grid. As an example, the ground state of diamond crystal is calculated using the ultrasoft pseudopotential. We discuss a numerical instability and a method of accelerating the convergence.

1 Introduction

Complex liquids could be defined as a general name of non-solidified condensed matters with hierarchal static and dynamical property under controlled circumstances. In complex liquids, the complexity stems from the cooperative or competitive property in atomic interaction, such as covalent interaction, ionic interaction, metallic interaction and hydrogen-bonded interaction. *Ab initio* electronic-structure calculations leads us to a unified picture of these properties. Therefore fundamental methodological improvements in the electronic-structure calculation are important to understand complex liquids.

After the success of Car and Parrinello in 1985 [1], *ab initio* molecular dynamics are applied to various systems; solid, liquid, amorphous, surface, and so on. The essentials of these success are (a) the self-consistent treatment of electron correlation within the local density approximation (LDA),[2] (b) the *ab initio* pseudopotential theories, (c) the plane-wave bases and the implementation of the Fast Fourier Transform (FFT), and (d) the progress of computer technologies such as vector processors, parallel processors or fast and cheap workstation. In the 90's, however, some limitations of the current framework are pointed out and one of them is the restriction on the system size. A typical system size is some hundreds of atoms in a periodic cell for silicon, or approximately one hundred atoms for other elements, which may allow restricted study of complex liquids. A difficulty for application to large systems is the system-size scaling. The present frame work is based on the plane-wave expansion of wavefunction, [1] and requires an $O(N^2 \log N)$ cost in CPU time in FFT procedures of the wavefunctions and an $O(N^3)$ cost in orthogonalization procedures of the wavefunctions. Here we denote N as the system size, the number of atoms or electrons in a periodic cell.

'Order-N' methods, or 'linear system-size-scaling' methods are so designed

that the total CPU time is $O(N)$, or linearly proportional to the system size. Nowadays 'Order-N' methods are possible within tight-binding Hamiltonian, but not yet in fully-selfconsistent case of the LDA calculation. Fortunately, the LDA Hamiltonian is a shortrange treatment of the electron-correlation, and so we could construct an 'order-N' scheme in principle, whereas the Hartree-Fock Hamiltonian requires $O(N!)$ CPU time to calculate the exchange potential.

For an 'order-N' scheme in LDA calculation, two issues are essential; one is a formulation without explicit orthogonalization or matrix-inversion procedures, because these procedures have an $O(N^3)$ CPU time. Mauri *et al.* [3] overcame this difficulty by introducing a new energy functional in the variational procedure called 'unconstrained minimization' (UM). The other issue is to construct a localized basis set. The current plane-wave method consumes an $O(N^2 \log_2 N)$ CPU time for the FFT procedures of plane-wave basis. [1] To avoid this computational cost, we could use local basis functions and such local basis functions, applicable to fully-selfconsistent calculations, may be given on a real-space grid. A DFT calculation with real-space regular grids is given by Chelikowsky and coworkers [4,5] and is called 'finite-difference (FD) real-space scheme'. In the FD real-space scheme, the kinetic-energy operator, or the Laplacian operator, must be a finite difference on real-space grids. In our previous works,[6,7] we constructed a foundation of the FD real-space scheme. However, this scheme is based on a global grid mesh in real space and could not be directly applied to the local-basis formulation.

This article is devoted to the methodology of our new formalism, towards the 'order-N' methods. In Section 2, we talk about the foundations of the FD real-space scheme, especially the *exact* kinetic-energy operator. [6] In Section 3, we summarize the original work of the UM minimization and demonstrate its example. In section 4, we give a generalization of the UM minimization to non-orthogonal localized bases. [11] In section 5, we propose a 'window function' technique so as to generate the localized basis function on a real-space grid, even within the non-local potential case. [11] In section 6, test calculations with the ultrasoft pseudopotential [8,9,10] are done on the ground state of diamond. [11] In section 7, we discuss the numerical instability of this scheme and a way to accelerate the convergence to the ground state.

In section 8, we summarize our work and comment further studies.

2 Foundation of finite-difference real-space scheme : kinetic-energy operator and preconditioning operator

In this section, the foundations of the FD real-space scheme are given, using the equivalence between basis sets in real and reciprocal space[6]. These foundations

are *not* directly related to the 'order-N' method, but are important to obtain results equivalent to the plane-wave based formalism. In our previous work [6], we introduce an *exact* kinetic-energy operator and a preconditioning operator as real-space finite differences. Here we omit, however, the latter topic and focus on the kinetic-energy operator.

In finite-difference real-space schemes, the kinetic-energy operator, is usually written as finite differences in real space. These FD formulas contain appreciable errors in case of finite mesh interval in real space. For instances, the 3-point FD and 5-point FD are, respectively,

$$\phi''(x) \approx \frac{1}{h^2}\big[-2\phi(x) + \{\phi(x+h) + \phi(x-h)\}\big] + O(h^2) \tag{1}$$

$$\phi''(x) \approx \frac{1}{h^2}\big[-30\phi(x) + 16\{\phi(x+h) + \phi(x-h)\} - \{\phi(x+2h) + \phi(x-2h)\}\big] + O(h^4). \tag{2}$$

Here, h corresponds to the mesh interval, and we discuss the 1-dimensional case for simplicity. Applications to 3-dimensional cases are straightforward.

We could derive an *exact* FD formula , though long-ranged , under the assumption that wavefunctions have a cutoff wavenumber in reciprocal space, just as in the current plane-wave scheme;

$$\phi(x) = \sum_{j=-J}^{J} c_j \exp\left(i\frac{2\pi}{L}x\right) = \sum_{|g|\le\pi/h} c_g e^{igx}, \quad \left(g = g_j \equiv \frac{2\pi}{L}j\right). \tag{3}$$

Here, L is the size of the periodic cell, and $2J \equiv L/h$ is the number of mesh points in one direction.

Using the discrete Fourier Transform $c_g = (h/L)\sum_n a_n e^{-ignh}$, where the summation over n means real-space integration, the wavefunction could be written exactly in real-space mesh grid.

$$\phi(x) = \sum_g c_g e^{igx} = \sum_g \frac{h}{L}\sum_n a_n e^{ig(x-nh)} = \sum_n a_n \tilde{\delta}(x-nh) \tag{4}$$

Here, the basis function $\tilde{\delta}(x)$

$$\tilde{\delta}(x) \equiv \frac{h}{L}\sum_{g\le\pi/h} c_g e^{igx} = \frac{h}{L}\sum_{j=-J}^{J} \exp\left(i\frac{2\pi}{L}x\right) = \frac{h}{L}\frac{\sin\left(\frac{\pi}{h}x\right)}{\sin\left(\frac{\pi}{L}x\right)} \tag{5}$$

could be called a 'delta function on mesh', because of the property $\tilde{\delta}(x{=}nh) = \delta_{n,0}$. An example is shown in the Fig. 1(a). The orthogonality of the bases $\{\tilde{\delta}(x-nh)\}_n$ could be shown as follows;

$$\int_0^L \frac{dx}{h}\tilde{\delta}^*(x-nh)\tilde{\delta}(x-n'h) = \left(\frac{h}{L}\right)^2 \sum_{g,g'} \int_0^L \frac{dx}{h} e^{-ig(x-nh)} e^{+ig'(x-n'h)}$$

$$= \left(\frac{h}{L}\right)^2 \sum_{g,g'} e^{i(gn-g'n')h} \int_0^L \frac{dx}{h} e^{-i(g-g')x)} = \left(\frac{h}{L}\right)^2 \sum_{g,g'} e^{i(gn-g'n')h} \delta_{g,g'}$$

$$= \frac{h}{L}\sum_{g'} e^{ig(n-n')h} = \tilde{\delta}((n-n)h) = \delta_{n,n'}. \qquad (6)$$

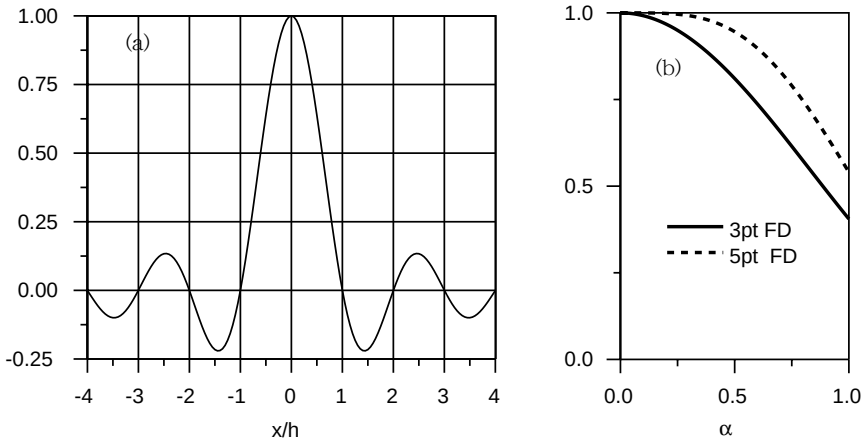

Figure 1: (a) The 'delta function' on mesh point $\tilde{\delta}(x)$, where $L/h = 16$. (b) The forms of the 'low-pass' filters, which correspond to the 3-point and 5-point FD, respectively.

Under the assumption (3) or (4), the matrix element of the kinetic-energy, is *exactly* written in a form on real-space mesh as

$$< \phi_1|\hat{\mathrm{T}}|\phi_2 >= \sum_{\mathrm{n,n'}} \mathrm{a}^*_{1\mathrm{n}}\mathrm{a}_{2\mathrm{n}}\mathrm{hT(n-n')}, \qquad (7)$$

where the transfer matrix $T(n-n')$ is

$$T(n-n') \equiv -\frac{1}{2}\int_0^L \frac{dx}{h}\tilde{\delta}^*(x-nh)\tilde{\delta}''(x-n'h)$$

$$= -\frac{1}{2}\left(\frac{h}{L}\right)^2 \sum_{g,g'} (-ig')^2 \int_0^L \frac{dx}{h} e^{-ig(x-nh)} e^{+ig'(x-n'h)}$$

$$= -\frac{1}{2}\frac{h}{L}\sum_{g} (-ig)^2 e^{ig(n-n')h} = -\frac{1}{2}\tilde{\delta}''((n-n)h). \tag{8}$$

The explicit form of $\tilde{\delta}''(x)$ and numerical tests of the accuracy of this *exact* kinetic-energy operator are given in our previous work [6].

We note that the low-order FD formula, such as the 3-point FD (1) and 5-point FD (2), could be interpreted as a 'low pass-filter ' in Fourier transform. For instances, the 3-point FD (1) and 5-point FD 2 correspond, respectively, to

$$\phi(x) = \sum_{|g|<\pi/h} \sigma(gh) e^{igx} c_g \tag{9}$$

$$\sigma(\alpha) \equiv \frac{2(1-\cos\alpha)}{\alpha^2} \tag{10}$$

and,

$$\sigma(\alpha) \equiv \frac{15 - 16\cos\alpha + \cos 2\alpha}{6\alpha^2} \tag{11}$$

The forms of the 'low-pass' filters are shown in Fig. 1(b).

These 'low-pass' filters are essentially equal to the Lanczos convergence technique in the numerical analysis, [12] which is introduced to suppresses the Gibbs phenomenon oscillations in the Fourier series.

3 Unconstrained Minimization 1 : Original work

In this section, we briefly summarize the original UM technique [3] before our generalization in the next section. In the DFT theory [2] with orthogonal basis orbitals $\{\psi\}$, the total electronic energy $E_{\rm tot}$ is

$$E_{\rm tot} \equiv 2\sum_{k}^{N} \left\langle \psi_k \left| \hat{T} + \hat{V}_{\rm NL}^{\rm ion} \right| \psi_k \right\rangle + E_{\rm LHXC}[n], \tag{12}$$

$$E_{\rm LHXC}[n] \equiv \int d\boldsymbol{r} V_{\rm loc}^{\rm ion}(\boldsymbol{r}) n(\boldsymbol{r}) + \frac{1}{2}\int\int d\boldsymbol{r} d\boldsymbol{r}' \frac{n(\boldsymbol{r})n(\boldsymbol{r}')}{|\boldsymbol{r}-\boldsymbol{r}'|} + E_{\rm XC}[n]. \tag{13}$$

Here, $2N$ is the total (valence) electron number per periodic cell and the charge density $n(\boldsymbol{r})$ is defined as

$$n(\boldsymbol{r}) \equiv 2\sum_{k}^{N} \psi_k^*(\boldsymbol{r})\psi_k(\boldsymbol{r}), \tag{14}$$

and the integration $\int n(\boldsymbol{r})d\boldsymbol{r} = 2\mathrm{Tr}[S] = 2\sum_k^N S_{kk}$ is always equal to the correct value $2N$. The orthogonalization constraint $S_{ij} \equiv <\psi_i|\psi_j> = \delta_{ij}$ should be satisfied in the variational procedure, so this formalism requires an explicit orthogonalization procedure, such as the Lagrange-multiplier technique or the Gram-Schmidt technique, which consumes an $O(N^3)$ CPU time. Hereafter we call this formalism the 'constrained minimization'.

The UM technique [3] was proposed so as to release the orthogonalization constraint and omit explicit orthogonalization steps in the variational procedure. This fundamental idea is based on a new variational procedure without any explicit orthogonalization procedure, and introduces a new energy functional $E_{\mathrm{tot}}^{\mathrm{UM}}$

$$E_{\mathrm{tot}}^{\mathrm{UM}} \equiv 2\sum_{ij}^{N} A_{ij} \left\langle \psi_i \left| \hat{T} + \hat{V}_{\mathrm{NL}}^{\mathrm{ion}} \right| \psi_j \right\rangle + E_{\mathrm{LHXC}}[n] + E_{\mathrm{UM}}, \tag{15}$$

$$E_{\mathrm{UM}} \equiv 2\mu\Delta N, \tag{16}$$

$$\Delta N \equiv N - \sum_{ij}^{N} A_{ij}S_{ij} = \sum_{ij}^{N} |S_{ij} - \delta_{ij}|^2 . \tag{17}$$

Here, the matrix A_{ij} is defined as $A_{ij} \equiv 2\delta_{ij} - S_{ji}$ or $A^t = 2I - S$ and I is the unit matrix. The charge density is redefined as

$$n(\boldsymbol{r}) \equiv 2\sum_{ij}^{N} A_{ij}\psi_i^*(\boldsymbol{r})\psi_j(\boldsymbol{r}), \tag{18}$$

and their integration $\int n(\boldsymbol{r})d\boldsymbol{r}$ is *not necessarily* equal to the correct value $2N$. The parameter μ must be appropriately chosen, and Mauri *et al.* [3] showed that the energy functional $E_{\mathrm{UM}}^{\mathrm{tot}}$ has the DFT ground state energy E_{GS} as its absolute minimum ($E_{\mathrm{UM}}^{\mathrm{tot}} \geq E_{\mathrm{GS}}$), when the parameter μ is chosen to be larger than the highest occupied level ($\mu > \epsilon_N$).

Here, we make some comments on the UM formalism. (i) Once the matrix A is set to be $A^t = S^{-1}$, the formalism is equivalent to the 'constrained minimization' formalism, and requires an $O(N^3)$ CPU time in matrix-inversion procedures, instead of explicit orthogonalization procedures. (ii) The definition $A^t \equiv 2I - S$ corresponds to the lowest expansion of the series $S^{-1} = \{I - (I - S)\}^{-1} = I + (I - S) + (I - S)^2 + (I - S)^3 + ...$ (iii) The minimization of the term $E_{\mathrm{UM}} \equiv 2\mu\Delta N$ in the energy functional (15) requires an iterative orthogonalization procedure ($S_{ij} \rightarrow \delta_{ij}$). When orthogonalization is achieved ($S_{ij} = \delta_{ij}$ thus $A_{ij} \equiv 2\delta_{ij} - S_{ji} = \delta_{ij}$), the minimization of E_{UM} is, again, identical to the 'constrained minimization' formalism

and requires neither explicit orthogonalization procedures nor matrix-inversion procedures. (iv) The quantity $2\Delta N \equiv 2N - 2\sum_{ij}^{N} A_{ij} S_{ij} = 2N - \int n(\boldsymbol{r}) d\boldsymbol{r}$ is the deviation of the charge from the correct value, and so one may call the energy functional (15) a 'ground-canonical like' potential and the parameter μ a 'chemical-potential like' parameter.

Figure 2 shows the variational procedure to the ground state of oxygen molecule, where we could find that the deviation of the total charge $2\Delta N$ is not zero under the course of the variational procedure.

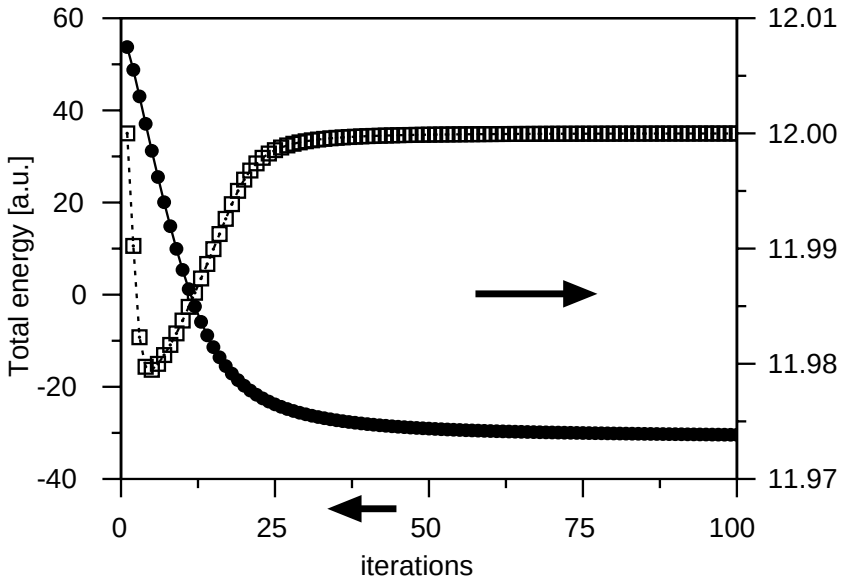

Figure 2: The total energy and the total electron number as a function of the number of iterations for the UM energy minimization. The calculation is done on oxygen molecule using the FD real-space scheme and the unconstrained minimization without localized bases. The correct total electron number in this system is 12.

4 Unconstrained Minimization 2 : Generalization

The original UM procedure [3] can be generalized to the framework of the localized basis orbitals. We expand the physical orbitals $\{\psi\}$, or the valence wavefunctions, into localized basis orbitals $\{\phi\}$, just as in the linear combina-

tion of atomic orbitals (LCAO) approximation,

$$\psi_i(\boldsymbol{r}) = \sum_{i'}^{M} c_{ii'} \phi_{i'}(\boldsymbol{r}). \tag{19}$$

Here $\{\phi\}$ are basis orbitals localized in real space and assumed to be centered on atomic sites. The total number of the localized basis orbitals $\{\phi\}$, M, is not necessarily equal to the number of occupied one-electron states N. We chose $M = 2N$ in our test calculation, which is discussed later. When we substitute Eq. (19) into Eq. (15), (17) and (18), we obtain, respectively,

$$E_{\rm UM}^{\rm tot} \equiv 2 \sum_{ij}^{M} B_{ij} \left\langle \phi_i \left| \hat{T} + \hat{V}_{\rm NL}^{\rm ion} \right| \phi_j \right\rangle + E_{\rm LHXC}[n] + E_{\rm UM}, \tag{20}$$

$$E_{\rm UM} \equiv 2\mu\Delta N, \tag{21}$$

$$\Delta N \equiv N - \sum_{ij}^{M} B_{ij} S_{ij}\,, \tag{22}$$

and

$$n(\boldsymbol{r}) \equiv 2 \sum_{ij}^{M} B_{ij}\, \phi_i^*(\boldsymbol{r}) \phi_j(\boldsymbol{r}). \tag{23}$$

Here, matrix B_{ij} is defined as $B_{ij} \equiv \sum_{i',j'}^{N} c_{i'i}^* c_{j'j} A_{i'j'}$ and $\int n(\boldsymbol{r}) d\boldsymbol{r} = 2{\rm Tr}\,[B^t S] = 2\sum_{ij}^{M} B_{ij} S_{ij}$. This energy functional is similar to that by Hernández *et al.*,[13] based on the density matrix approach with a model local potential. The only difference in the energy functional is the form of B_{ij} or a choice of variational parameters in the actual procedure. One should refer to a comment on this point in section IIC of their paper [13].

Note that in our actual test calculation with the ultrasoft pseudopotential,[8,9,10] the definitions (14), (18) and (23) are also replaced, respectively, by $n(\boldsymbol{r}) \equiv 2\sum_{k}^{N} \left\langle \psi_k \left| \hat{S}(\boldsymbol{r}) \right| \psi_k \right\rangle$, $n(\boldsymbol{r}) \equiv 2\sum_{ij}^{N} A_{ij} \left\langle \psi_i \left| \hat{S}(\boldsymbol{r}) \right| \psi_j \right\rangle$ and $n(\boldsymbol{r}) \equiv 2\sum_{ij}^{M} B_{ij} \left\langle \phi_i \left| \hat{S}(\boldsymbol{r}) \right| \phi_j \right\rangle$, respectively. Here the operator $\hat{S}$ is defined [8] as

$$\left\langle \phi_i \left| \hat{S}(\boldsymbol{r}) \right| \phi_j \right\rangle \equiv \phi_i^*(\boldsymbol{r}) \phi_j(\boldsymbol{r}) + \sum_{Inm} Q_{nm}^I(\boldsymbol{r}) \left\langle \phi_i \middle| \beta_n^I \right\rangle \left\langle \beta_m^I \middle| \phi_j \right\rangle, \tag{24}$$

where I indicates an atom, and suffixes n and m indicate reference states in an atom. The charge density $n(\boldsymbol{r})$ is written, for instance, as

$$n(\boldsymbol{r}) \equiv 2\sum_{k}^{N} \left\langle \psi_k \left| \hat{S}(\boldsymbol{r}) \right| \psi_k \right\rangle$$
$$\equiv 2\sum_{k}^{N} |\psi_k(\boldsymbol{r})|^2 + \sum_{Inm} Q^I_{nm}(\boldsymbol{r}) \sum_{ki}^{N} \left\langle \psi_k \middle| \beta^I_n \right\rangle \left\langle \beta^I_m \middle| \psi_k \right\rangle . \quad (25)$$

The overlap matrix S_{ij} is redefined as

$$S_{ij} \equiv \int d\boldsymbol{r} <\phi_i|\hat{S(\boldsymbol{r})}|\phi_j> \equiv <\phi_i|\phi_j> + \sum_{Inm} q^I_{nm} \left\langle \phi_i \middle| \beta^I_n \right\rangle \left\langle \beta^I_m \middle| \phi_j \right\rangle , \quad (26)$$

where $q^I_{nm} = \int d\boldsymbol{r} Q^I_{nm}(\boldsymbol{r})$. See the original work [8] for more details.

5 Window-function technique

In this section, we explain how to generate localized basis orbitals within the FD real-space scheme. To construct localized orbitals on a real-space regular grid, we adopt a window-function technique, which allows us to optimize the forms of localized basis orbitals instead of fixing them. A localized orbital ϕ_i could be generated from an extended orbital $\bar{\phi}_i$ by

$$\phi_i(\boldsymbol{r}) \equiv w_i(\boldsymbol{r})\bar{\phi}_i(\boldsymbol{r}). \quad (27)$$

Here, we introduce a *window* function w_i to localize basis orbitals within a spherical region around an ion. The form of a window function must depend only on the distance from the ion position $\boldsymbol{R}$ that the localized orbital belongs to, *i.e.* , $w(\boldsymbol{r}) = w(|\boldsymbol{r} - \boldsymbol{R}|)$, and is zero outside the local 'cell', *i.e.* , $w(|\boldsymbol{r} - \boldsymbol{R}|) = 0(|\boldsymbol{r} - \boldsymbol{R}| > R_{\rm L})$. The parameter $R_{\rm L}$ is the radius of the local cell.

The implementation of a window function guarantees the locality of ϕ_i in a spherical local-cell region ($|\boldsymbol{r} - \boldsymbol{R}| < R_{\rm L}$) and satisfies the (Dirichlet) boundary condition, because the energy variation with respect to $\bar{\phi}$ is reduced to

$$\frac{\delta E}{\delta \bar{\phi}_i(\boldsymbol{r})} = \frac{\delta \phi_i(\boldsymbol{r})}{\delta \bar{\phi}_i(\boldsymbol{r})} \frac{\delta E}{\delta \phi_i(\boldsymbol{r})} = w_i(\boldsymbol{r}) \frac{\delta E}{\delta \phi_i(\boldsymbol{r})}. \quad (28)$$

In our calculation, we use the ultrasoft pseudopotential, where $(\hat{T} + \hat{V}^{\rm ion}_{\rm NL})|\phi\rangle$ is not localized in a local cell. Therefore this formalism of the window function is essential to optimize the localized basis orbitals on a regular grid.

The resultant variational procedure should be achieved with respect to $\{\bar{\phi}\}$ and $\{c_{ii'}\}$. The variations with respect to the orbitals $\{\bar{\phi}\}$ correspond to the optimization of the local basis function on a real-space regular grid and those with respect to the coefficients $\{c_{ii'}\}$ correspond to the determination of eigen states. Though $\bar{\phi}$ is, in principle, an extended function, its components in the outer region ($|\boldsymbol{r} - \boldsymbol{R}| > R_{\rm L}$) do not contribute to the total energy and so we can neglect these components in actual computational procedures.

The window-function technique is also advantageous in force calculations, which is important in a molecular-dynamics simulation. Because a localized orbital ϕ depends on the position of the ion $\boldsymbol{R}$ only through the window function $w(|\boldsymbol{r} - \boldsymbol{R}|)$, the derivatives of orbitals with respect to positions of ions are reduced to

$$\frac{\partial \phi_i(\boldsymbol{r})}{\partial \boldsymbol{R}} = \frac{dw_i(\boldsymbol{r})}{d\boldsymbol{R}} \bar{\phi}_i(\boldsymbol{r}), \tag{29}$$

which could make calculations of the Pulay force straightforward.

6 Test calculations on diamond

We tested the present formalism numerically on the ground state of diamond crystal, using the ultrasoft pseudopotential[8,9,10] and the local-density approximation (LDA) with the Perdew-Zunger exchange-correlation potential,[14] and used the cubic supercell containing 8 atoms, where the edge length of a periodic cell L is $L = 6.727$ atomic unit (a.u.). We use the double-grid technique in the ultrasoft pseudopotential,[8,9,10] where the spacings of the real-space grid h are $h = 0.42$ a.u. for orbitals and 0.21 a.u. for the charge density. For the reference states in the ultrasoft pseudopotential, one reference energy is adopted for each angular momentum l.[10] As in our previous works of the FD real-space scheme,[6,7] FFT procedures are used to generate the potential from the charge density $n(\boldsymbol{r})$. These FFT procedures consumes negligible CPU time, whereas, in the current plane-wave scheme, FFT procedures of all orbitals dominate CPU time.

Four localized orbitals ϕ_i for each atom are prepared, and are optimized in the variational procedure of Eq. (20). The number of valence orbitals $\{\psi\}$ for a carbon atom is two, and so the choice of four localized basis orbitals $\{\phi\}$ per atom corresponds to $M = 2N$. Their initial forms of ϕ_i are chosen to be (s-, p_x-, p_y-, p_z-) atom-centered Gaussian forms, as those in Hernández *et al.* The explicit forms of s- and p_z- Gaussians, for instance, are $\bar{\phi}_{\rm s} = \exp(-r^2/R^2)$ and $\bar{\phi}_{\rm p_z} = z\exp(-r^2/R^2)$, respectively. The width of Gaussian R is determined to reproduce the peak of the radial component of the atomic pseudowavefunction, and the optimal value is roughly estimated to $R = 2.018$ a.u. Results are not

sensitive of the detail in the choice of R, because the wavefunctions $\bar{\phi}$ have components only on the mesh points. A window function $w(r)$ is chosen as $w_i(r) \equiv \cos(\frac{\pi}{2}\frac{r}{R_L})$ inside a local cell ($r < R_L$), and $w_i(r) \equiv 0$ outside ($r > R_L$). The radius of the local cell R_L is $R_L = 3.3635$ a.u.

The resultant ground-state energy per atom E is $E = 5.602$a.u./atom, which agrees satisfactorily with the value of $E = 5.617$a.u./atom in our previous work, [10,7] calculated using the FD real-space scheme without localized orbitals. For comparison, we also calculated using 'fixed' local basis orbitals, where localized orbitals $\{\phi\}$ are fixed to be the initial Gaussian forms and only coefficients $\{c_{ii'}\}$ are optimized in the variational procedure. The resultant ground state energy $E = 5.204$a.u./atom is worse than the result calculated with optimized $\{\phi\}$. Therefore, the optimization of $\{\phi\}$ is crucial and we should retain the possibility of the optimization of the localized orbitals $\{\phi\}$.

Figure 3 (a) shows the charge density of diamond in (110) plane. It can be seen that characteristic two peaks of the charge density $n(\mathbf{r})$ appear between bonding carbon atoms. [10,15] Figure 3 (b) shows the charge density in the [001] direction. Here we, again, comment that the charge density in the ultrasoft pseudopotential are decomposed into the following two part; the 'soft' charge of the pseudo wavefunctions, the first term in (25), and the augmentation charge, the second term in (25).

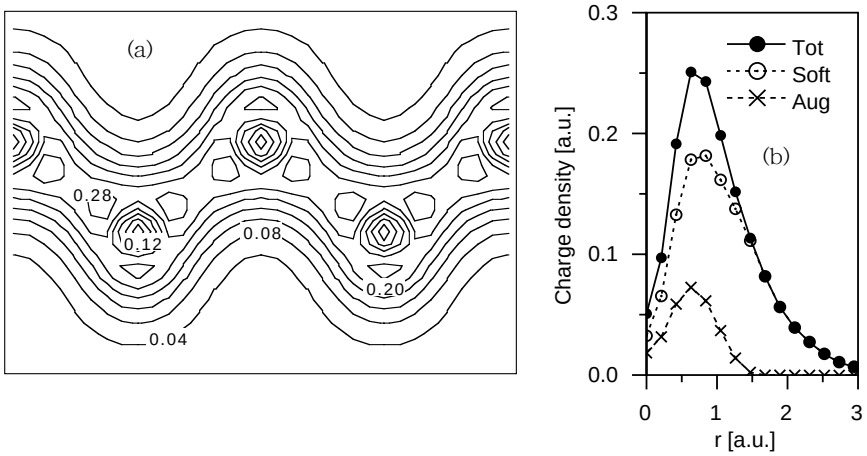

Figure 3: (a) Charge density of diamond on (110) plane. Contours are plotted in every 0.04 a.u. (b) Charge density in [001] direction; the total charge density, the 'soft' charge density contributed only by pseudo-wavefunctions, and the augmentation charge. See detail in the text.

Figure 4 shows the resultant or optimized form of $\{\phi\}$ on a real-space mesh. It is clear that the initially s-Gaussian orbital keeps the s-symmetry in the ground state, while the initially p_z-Gaussian orbitals are mixed with p_x- and p_y- Gaussian orbitals. In Fig. 4(a), the lack of the charge within $r < 1.5$ a.u. could be seen and corresponds to the lack of the augmention charge in Fig. 3.

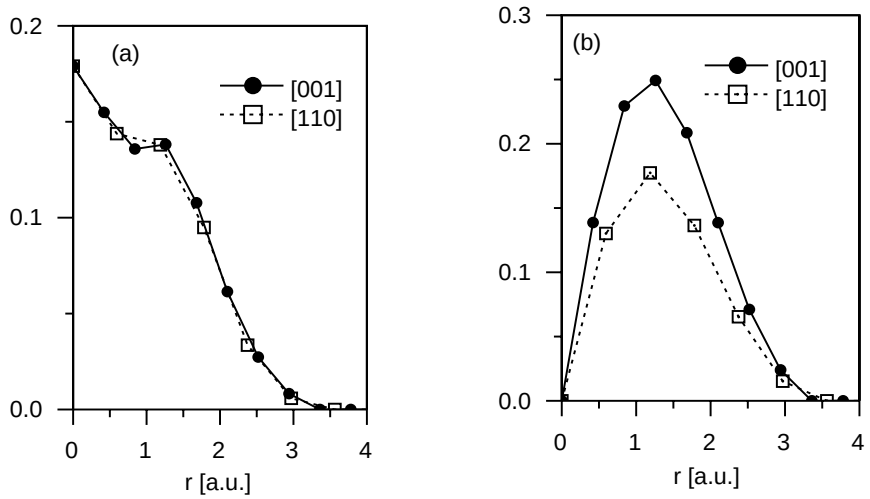

Figure 4: Localized basis orbitals $\{\phi\}$ in diamond crystal, optimized by the present variational procedure: (a) initially s-Gaussian (b) initially p_z-Gaussian. The orbitals $\{\phi\}$ are normalized.

7 Avoiding the numerical instability and accelerating the convergence in UM

Finally, we comment on a numerical stability of our scheme. As already discussed in Section 3, the UM scheme breaks the charge neutrality $2\Delta N \equiv 2N - \int n(\boldsymbol{r})d\boldsymbol{r} \neq 0$ in the course of the variational procedure, which may cause a numerical instability in the Hatree (or Coulomb) energy.

We could avoid this numerical instability by the additional iterative orthogonalization, or the minimization of $E_{\rm UM} \equiv 2\mu\Delta N$ with respect to the coefficients $c_{ii'}$, which consumes negligible CPU time. This iterative orthogonalization leads to the orthogonality in any accuracy using the convergence criteria for $E_{\rm UM}$ ($E_{\rm UM} < E_{\rm UM}^{(c)}$). By setting $E_{\rm UM}^{(c)} = 0$, we could achieve the perfect orthogonalization, numerically, but, such 'perfect ' orthogonalization causes poor convergence to the ground state. So we found an optimal criteria $E_{\rm UM}^{(c)}$ to be the smaller quantity of (1) 10 % of the energy deviation of the total energy from the last iteration, $|E_{\rm tot}^{(n)} - E_{\rm tot}^{(n-1)}|$ and (2) 1 % of the present total energy $E_{\rm tot}^{(n)}$.

Figure 5 demonstrates that the present 'imperfect ' orthogonalization with the optimal $E_{\rm UM}^{(c)}$ accelerates the convergence, compared with the case with the perfect orthogonalization $E_{\rm UM}^{(c)} = 0$.

8 Summary and discussion

In summary, we construct foundations for a fully-selfconsistent 'order-N' scheme, within the FD real-space scheme. The essential foundations are (i) the variational principle with respect to nonorthogonal localized orbitals and (ii) the construction of localized orbitals on real-space regular grids. The former issue is resolved by application of the UM technique to the nonorthogonal basis set and the latter issue is resolved by introducing a window function to localize basis orbitals. The formulation is tested numerically on the ground state of diamond crystal with ultrasoft pseudopotential and shows satisfactory agreement with conventional methods.

We must note that the present formulation is an intermediate scheme between a tight-binding formalism and a fully-selfconsistent (DFT) formalism with a complete basis set, in the sense that, if we fix basis orbitals $\{\phi\}$ and the Hamiltonian, the formalism is reduced to the tight-binding formulation. One interesting application of the present formalism is calculations with 'partially fixed' basis orbitals. For many calculations, such as surface structures and defects in solids, almost all atoms, except those near a surface or a defect, are the same as in a bulk system. In such a 'bulk' or 'buffer' region, localized basis

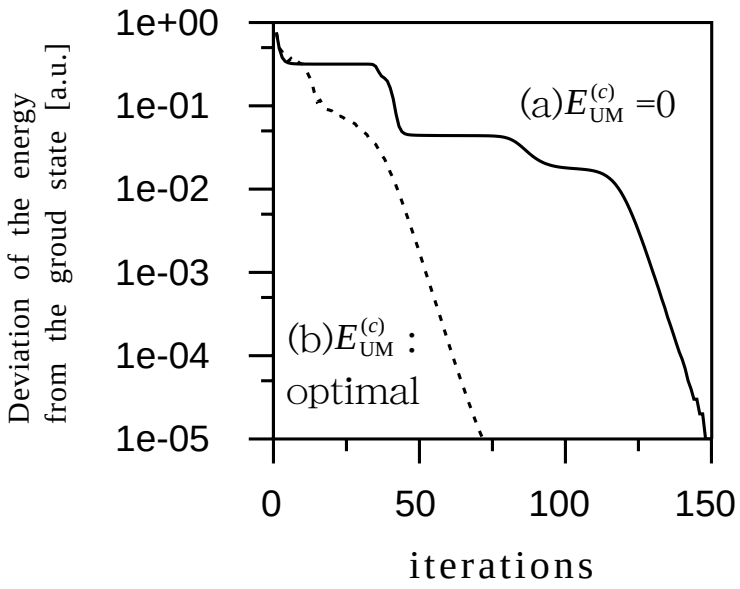

Figure 5: Effect of the additional iterative orthogonalization with respect to the coefficient $c_{ii'}$. The rate of convergence using (a) 'perfect' orthogonalization, setting $E_{\rm UM}^{(c)} = 0$, (b) 'perfect' orthogonalization with optimal $E_{\rm UM}^{(c)}$. The basis functions $\{\phi\}$ are fixed.

orbitals could be fixed to be 'bulk' states in a good approximation. This saves CPU time and memory space for computation. Even in this case, the calculation can be fully-selfconsistent, because the Hamiltonian is exactly equal to that of the DFT with no parameters.

Acknowledgments

This work is supported by Special Coordination Funds for Promoting Science and Technology, by a Grant-in-Aid for COE Research and also by a Grant-in-Aid from the Japan Ministry of Education, Science, Sports and Culture. The numerical calculation was carried out by the computer facilities at the Institute

of Molecular Science at Okazaki and at the Institute for Solid State Physics at the University of Tokyo.

References

1. R. Car and M. Parrinello, Phys. Rev. Lett. **55**, 2471 (1985). For review articles, D. K. Remler and P. A. Madden, Mol. Phys. **70**, 921 (1990); M. C. Payne, M. P. Teter, D.C. Allan, T. A. Arias and J. D. Joannopoulos, Rev. Mod. Phys. **64**, 1045 (1992).
2. P. Hohenberg and W. Kohn, Phys. Rev. **136B**, 864 (1964); W. Kohn and L. J. Sham, Phys. Rev. **140**, A1133 (1965). For review articles, R. O. Jones and O. Gunnarsson, Rev. Mod. Phys. **61** , 689 (1989).
3. F. Mauri, G. Galli and R. Car, Phys. Rev. B **47**, 9973 (1993); F. Mauri and G. Galli, Phys. Rev. B **50**, 4316 (1994); J. Kim, F. Mauri and G. Galli, Phys. Rev. B **52**, 1640 (1995).
4. J. R. Chelikowsky, N. Troullier and Y. Saad, Phys. Rev. Lett. **72**, 1240 (1994); J. R. Chelikowsky, N. Troullier, K. Wu and Y. Saad, Phys. Rev. B **50**, 11355 (1994).
5. X. Jing, N. Troullier, D. Dean, N. Binggeli, J. R. Chelikowsky, K. Wu and Y. Saad, Phys. Rev. B **50**, 12234 (1994).
6. T. Hoshi, M. Arai, and T. Fujiwara, Phys. Rev. B **52**, R5459, (1995).
7. T. Hoshi, and T. Fujiwara, in *Frontier in Material Modeling and Design*, Edited by B. Raj and V. Kumar, pp. 51-58, Springer Verlag, Heidelberg (1997).
8. D. Vanderbilt, Phys. Rev. B **41**, 7892 (1990); K. Laasonen, R. Car, C. Lee and D. Vanderbilt, Phys. Rev. B **43**, 6796 (1991).
9. K. Laasonen, A. Pasquarello, R. Car, C. Lee and D. Vanderbilt, Phys. Rev. B **47**, 10142 (1993).
10. T. Fujiwara, and T. Hoshi, J. Phys. Soc. Jpn, **66**, 1723 (1997).
11. T. Hoshi, and T. Fujiwara, to be published in J. Phys. Soc. Jpn. **66**, No.12 (1997).
12. C. Lanczos, *Applied Analysis*, Englewood Cliffs, New Jersey: Prentice-Hall (1956).
13. H. Hernández, M.J. Gillan, and C.M. Goringe, Phys. Rev. B **53**, 7147, (1996).
14. J. P. Perdew and A. Zunger, Phys. Rev. B **23**, 5048 (1981).
15. M. T. Yin and M. L. Cohen, Phys. Rev. **B24**, 6121 (1981).